

NGU Report 97.009

Environmental investigation of two stations
from the Snorre field, Tampen area, 1996

Report no.: 97.009		ISSN 0800-3416	Grading: Open
Title: Environmental investigation of two stations from the Snorre field, Tampen area, 1996			
Authors: Terje Thorsnes, Heidi A. Olsen & Reidulv Bøe		Client: Saga Petroleum	
County:		Commune:	
Map-sheet name (M=1:250.000)		Map-sheet no. and -name (M=1:50.000)	
Deposit name and grid-reference:		Number of pages: 32	Price (NOK):
		Map enclosures:	
Fieldwork carried out: June 1996	Date of report: 10.01.1997	Project no.: 2664.08	Person responsible: <i>Eystein Nordgulen</i>
<p>Summary:</p> <p>Cores from two stations in the Tampen area, in the Norwegian Trench west of Florø, have been analysed (geochemistry, sedimentology, physical properties) and dated (²¹⁰Pb-dating). One station was located 1000 m downstream, northeast of the Snorre field, while the other (reference) station was located 9 km to the east-northeast of the Snorre field.</p> <p>The downstream station was clearly influenced by drilling mud discharges, with elevated levels of Ba and Pb in the top sediments. Discrepancies between reported discharges and contaminant contents at dated sediment intervals indicated that resuspension or changing oceanographic conditions may influence the sedimentary record of contaminant discharges.</p> <p>Elevated levels of Ba and Pb in the reference station indicate spreading of drilling-related contaminants over considerable areas.</p> <p>Comparatively high levels of trace metals in old sediments not influenced by anthropogenic inputs demonstrates the importance of geological control in environmental monitoring.</p> <p>Keywords: Snorre, Tampen, environment, geochemistry, dating, sedimentology</p>			
Keywords: Geokjemi	Datering	Sedimentologi	
Miljøgeologi			

CONTENTS

1. INTRODUCTION.....	4
2. METHODS.....	4
2.1 Handling of cores	4
2.2 X-ray investigation	5
2.3 Sub-sampling.....	5
2.4 Cores/samples for storage.....	5
2.5 Geochemical analysis	5
2.6 Grain-size analysis.....	6
2.7 Sedimentological description	6
2.8 Density measurements.....	6
2.9 Pb-dating.....	7
3. DESCRIPTION AND RESULTS	7
3.1 Sedimentology and physical properties.....	7
3.2 Pb-dating.....	9
3.3 Geochemistry.....	9
4. DISCUSSION AND CONCLUSIONS.....	11
5. REFERENCES	15

FIGURES

- Fig. 1. Location map.
- Fig. 2a. Dry bulk density, both cores.
- Fig. 2b. Median diameter, both cores
- Fig. 3. Grain-size distribution for all samples in the S-TLP-3C and R1-B cores.
- Fig. 4. Estimates of sedimentation rates. A: core S-TLP-3A. B: core R1-A.
- Fig. 5. Year AD versus depth in cores.
- Fig. 6. ¹³⁷Cs levels in the S-TLP-3A core.
- Fig. 7. Bivariate plot of Cu, Pb, Zn, Hg, Ba and TOC versus the core depth, core S-TLP-3A.
- Fig. 8. Bivariate plot of Cu, Pb, Zn, Hg, Ba (and TOC) normalised against TOC, core S-TLP-3A.
- Fig. 9. Bivariate plot of Cu, Pb, Zn, Hg, Ba and TOC normalised against grain-size, core S-TLP-3A.
- Fig. 10. Bivariate plot of Cu, Pb, Zn, Hg, Ba and TOC versus the core depth, core R1-A.
- Fig. 11. Bivariate plot of Cu, Pb, Zn, Hg, Ba (and TOC) normalised against TOC, core R1-A.
- Fig. 12. Bivariate plot of Cu, Pb, Zn, Hg, Ba and TOC normalised against grain-size, core R1-A.
- Fig. 13. Bivariate (stratigraphic) plot of Cu, Pb, Zn, Hg, Ba and TOC versus a time axis in years, based on Pb-dating. Both cores are shown.

TABLES

Table 1 Geochemical analyses, grain-size, age and physical properties

1. INTRODUCTION

The purpose of this investigation has been to evaluate to what extent the drilling discharges accumulate in the Tampen area, or are resuspended and transported out of the area. In order to study this, we have looked at the temporal and spatial distribution of contaminants related to discharges from the Snorre field in particular, and more diffuse discharges related to drilling and production in a wider area. The report presents data and interpretations from cores retrieved at 2 stations (S-TLP-3, R1; Fig. 1) in the vicinity of the Snorre field, which is situated in the blocks 34/4 and 34/7 in the Norwegian sector of the North Sea 150 km west of Florø and 20 km northeast of the Statfjord platform. The cores were collected by DNV/SINTEF during June 1996, as part of the 1996 monitoring survey of the Tampen area.

Exploration drilling was undertaken in the period March 1980 to November 1986 (three wells). Production drilling on the TLP (Tension Leg Platform) started in 1990, and has been more or less continuous since the Snorre platform was installed in May 1992. A total of 25 wells has been drilled at the Snorre TLP. The drilling at the Subsea production system started in 1992 and continued until 1995, with a total of 12 wells.

One of the analysed stations (S-TLP-3) is located 1000 m downstream, northeast of Snorre, while the other (R1) station is located c. 9 km to the east-northeast of the Snorre field. The cores have been analysed with regard to sedimentological and geochemical parameters, and dated by the ^{210}Pb -method. The fact that only two stations have been studied limits the conclusions to be drawn from the investigation, but the data do show significant spatial and temporal trends reflecting contaminant discharges.

2. METHODS

2.1 Handling of cores

The cores were received in frozen condition; 2 cores from the reference station (labelled R1-A and R1-B by NGU), and 3 cores from the downstream station (labelled S-TLP-3A, S-TLP-3B and S-TLP-3C by NGU). Core diameter: 60 mm. The cores were thawed in vertical position prior to sub-sampling and sedimentological description (see below). The core lengths were: R1-A: 32.5 cm, R1-B: 35 cm, S-TLP-3A: 33 cm, S-TLP-3B: 30.5 cm and S-TLP-3C: 32.5 cm.

2.2 X-ray investigation

All cores were X-rayed in frozen condition. This investigation included description of sedimentary structures, clast content and transparency. All sections of the cores were recorded digitally, and these images (graphic files) are available.

2.3 Sub-sampling

Cores R1-A and S-TLP-3 were sub-sampled for geochemical analysis and Pb-dating by sub-sampling the upper 5 cm in 0.5 cm thick slices, and sub-sampling the deeper parts every 5 centimetres. The sub-samples were subsequently split in two; one for geochemical and one for dating purposes. The following slices were sampled: 0-0.5 cm, 0.5-1.0 cm, 1.0-1.5 cm, 1.5-2.0 cm, 2.0-2.5 cm, 2.5-3.0 cm, 3.0-3.5 cm, 3.5-4.0 cm, 4.0-4.5 cm, 4.5-5.0 cm, 10-10.5 cm, 15-15.5 cm, 20-20.5 cm, 25-25.5 cm and 30-30.5 cm. The ice plugs above the sediment/water interface had caused an undulating surface, which gave rise to problems for the sampling of the uppermost 0.5 cm intervals. Sub-samples for geochemical analyses were freeze-dried prior to further preparation.

Cores R1-B and S-TLP-3C were split in two halves along the core. One was used for sedimentological description and density measurements, while the other was sub-sampled for grain-size analysis.

2.4 Cores/samples for storage

Core S-TLP-3B was not opened, and will be stored in a cold room at NGU until further instructions are received from Saga. The core will be disposed of in July 1997 if no instructions are received from Saga within this date. Bulk samples from cores R1-B and S-TLP-3C have been collected and stored in the cold room in case of further analyses.

2.5 Geochemical analysis

All methods (below) are accredited according to NS-EN-45001. Sample preparation was carried out by drying at 50° C for 48 hours. After homogenisation, 1 g of material was extracted with 20 ml of 7N HNO₃ in closed borosilicate bottles at 120° C for half an hour, in accordance with Norwegian standard NS 4770. Cu, Zn and Ba were analysed by inductively

coupled plasma atomic emission spectrometry (ICP-AES) with a Jarrel-Ash Model 975 ICAP AtomComp. Pb was analysed by graphite furnace atomic absorption spectrometry with a Perkin Elmer Model SIMAA 6000 instrument. Hg was analysed by cold vapour atomic absorption spectrometry with a Perkin Elmer Model 403 instrument. The content of total organic carbon (TOC) was analysed by oxidation of carbon to CO₂ in a combustion furnace, type LECO SC-444. Prior to analyses, inorganic carbon from carbonates was removed by treating the sample with HCl.

2.6 Grain-size analysis

The method is accredited according to NS-EN-45001. The material was suspended in water and the organic material oxidised with H₂O₂ by heating in a water bath. After decantation, the clear solution was subsequently removed (de-salting). The residue was freeze-dried, and the dry sample sieved through a 2 mm sieve and prepared using ultra sound immediately prior to analysis. The grain-size analysis was carried out in a Coulter LS 200 which measure grain-size and grain-size distribution based on laser diffraction.

2.7 Sedimentological description

The sedimentological description included lithology, texture, sedimentary structures, colour and eventual disturbances in the core. Colour description was based on Munzell-Soil-Color-Charts. The description of colour was carried out immediately after the opening of the cores in order to avoid colour changes induced by drying and oxidisation of the core material.

2.8 Density measurements

Density measurements were carried out using a thin-walled metal ring with known weight and volume, which was carefully pressed into the sediment. The wet sample was immediately weighed, and the sample was subsequently dried at 105° C in 24 hours, before weighing of the dry material. Wet and dry bulk densities were calculated according to the following formulas:

Wet bulk density = weight wet sample/volume wet sample

Dry bulk density = weight dry sample/volume wet sample

2.9 Pb-dating

Pb-dating and geochemical analyses were carried out on splits of the same slices (see above for sub-sampling intervals). The Pb-datings were carried out by Dr. H. Kunzendorf at the Gamma Dating Centre, Risø national Laboratory, Roskilde. A reverse-electrode coaxial Ge detector (20 % rel. efficiency) with energy resolution values of 640 eV and 1.7 KeV at 5.9 KeV and 1332 KeV, respectively, was used. The gamma-ray spectra from the samples were collected by means of a normal nuclear counting apparatus (standard counting electronics and PC-based counting system). All the ^{210}Pb intensities (cps/kg dry weight) were calculated directly from the counting rate of the 46.5 keV peak. ^{137}Cs was determined from its 661.6keV peak. For further details regarding the analytical procedures, see e.g. Kunzendorf et al. 1996.

3. DESCRIPTION AND RESULTS

3.1 Sedimentology and physical properties

In both cores, two layers can be distinguished. The upper layer extends from the surface down to 15-20 cm, while the lower layer extends to the bottom of the cores. The two layers are evident in the sedimentological data. The contrasting sedimentological parameters of the two layers indicate a change in sedimentary regime at the boundary between the two layers. A hiatus of unknown duration is represented by the layer boundary. The age of the lower layer can not be determined with the methods used in this investigation.

Station S-TLP-3

X-ray investigations of the S-TLP-3 cores showed that the sediments in the 0-20 cm interval are bioturbated and contain small dark and light fragments in the matrix. A dark zone in the 2-3 cm interval may represent material enriched in organic matter. The sediments below 20 cm are massive and without structures, except in core S-TLP-3C where small dark fragments are present. Small ice needles occur in all cores below 20 cm.

Sedimentological, visual inspection of core S-TLP-3C showed that the upper 0-20 cm sediments are massive, clayey silt (colour 5Y-5/2) with 0.5-1 cm shell fragments. The sediments in the 20 - 35 cm interval are very dark gray (colour 5Y-3/1) massive, silty clays.

Density measurements of core S-TLP-3C are shown in Table 1. The wet bulk density increases downward (Fig. 2A), and the highest densities were recorded in the 15 - 20 cm interval (1.83 - 1.85 g/cm³). The density decreases in the 20 - 25 cm interval, and the wet bulk

density is 1.69 cm^3 at 25 cm. Dry bulk density follows the same trend, and is lowest at 25 cm, 1.05 g/cm^3 .

Grain-size analysis was carried out on core S-TLP-3C. The median diameters of the sediments in the 0-15 cm interval are in the 0.055-0.065 mm range, while the median diameters of the 20-35 cm interval are in the 0.010-0.015 mm range (Fig. 2B). The distribution of grain-sizes between 0.004 and 2 mm is shown in Fig. 3. The grain-size distribution showed a clear boundary at 20 cm. In the 0 - 20 cm interval, the sediments consisted of well-sorted coarse silt, while the sediments below (at 20-21 cm, 25-26 cm and 30-31 cm) are poorly sorted, with grain-sizes in the medium to coarse silt fraction, and a relatively large fraction of fine silt.

Station R1

X-ray investigations of the R1 cores showed that the sediments in the 0-20 cm interval of core R1-A are bioturbated, particularly in the 10-20 cm interval. The sediments in both cores below 20 cm were massive, with small dark fragments and abundant small ice needles.

Sedimentological, visual inspection of core R1-B showed that the upper 0-8 cm sediments were massive, gray clayey silt (colour 5Y-5/1). The sediments in the 8-21 cm interval consisted of alternating layers (0.5-1.5 cm thick) with gray clayey silt (colour 5Y-5/1) and very dark gray silty clay (colour 5Y-4/1). This alternation may be due to bioturbation. The sediments in the 21-36 cm interval consisted of massive, very dark gray silty clay (colour 5Y-4/1).

Density measurements from core R1-B are shown in Table 1. The wet bulk densities in core R1-B followed the same trend as in the core S-TLP-3C (Fig. 2A). The increase of wet bulk densities extended down to c. 15 cm where wet and dry bulk densities were 1.86 and 1.32 g/cm^3 , respectively. The densities decreased below this level, with wet bulk densities between 1.72 and 1.74 g/cm^3 , and dry bulk densities between 1.09 and 1.14 g/cm^3 .

Grain-size analysis was carried out on core R1-B. The distribution of grain-sizes between 0.004 and 2 mm is shown in Fig. 3. The grain-size distribution showed a two-fold division similar to the S-TLP-3C core, but with some fluctuations in the 15-20 cm interval. The transition from the coarse-grained material in the upper layer to more fine-grained in the lower layer was recorded at the 15-16 cm level, but the grain-size in the 20-21 cm interval is again more coarse-grained, with a clear peak in the coarse silt fraction. The fluctuating grain-sizes in this interval may be caused by primary variations in the sedimentary regime, but bioturbation or sediment disturbance may also be involved. The median diameters are 0.050 to 0.060 mm in the 0-10 cm interval, fluctuate between 10 and 20 cm, and range from 0.010 to 0.020 mm at the 25 and 30 cm levels (Fig. 2B).

3.2 Pb-dating

Dating of the S-TLP-3A and R1-A cores showed that continuous sedimentation has occurred in the time interval considered (1900 AD to the present), even though minor perturbations are evident.

Station S-TLP-3

The estimated linear sedimentation rate at the S-TLP-3 station is 1.35 mm/year. The estimated deposition year using the average of slice intervals (e.g. 0.25 cm for the 0-0.5 cm interval) is shown in Table 1. The estimated annual mass accumulation rate is 502 g/m², with a standard deviation of 70 g. The estimated sedimentation rates (Fig. 4A) indicate a generally stable sedimentation, even though some minor fluctuations appear to have occurred in the 1960-1990 interval. The general downward decrease of the sedimentation rate is related to sediment compaction. Estimated ages for core depths down to 10 cm are shown in Fig. 5. Measurement of ¹³⁷Cs-contents (Fig. 6) show a pronounced peak at the 1988 level which likely represents the emissions of radioactive material into the atmosphere from the Chernobyl accident in 1986. The other measurements are close to the detection limit, and no interpretations can be drawn from these.

Station R1

The estimated linear sedimentation rate at the R1-A station is 0.49 mm/year. The estimated deposition year using the average of slice intervals (e.g. 0.25 cm for the 0-0.5 cm interval) is shown in Table 1. The estimated annual mass accumulation rate is 347 g/m², with a standard deviation of 36 g. The estimated sedimentation rates (Fig. 4B) indicates a generally stable sedimentation, but with some irregularities. This may be caused by bioturbation, or some resuspension and mixing of the sediment. The general downward decrease of the sedimentation rate is related to sediment compaction. Estimated ages for core depths down to 5 cm are shown in Fig. 5. The levels of radioactive Pb at 10 cm was too low to yield meaningful results, and ages below 5 cm have therefore not been estimated. Measurement of Cs-contents yielded contents close to the detection limits, and no conclusions can be drawn from these data.

3.3 Geochemistry

The geochemical data showed clear differences between the two stations, with clearly elevated levels of Ba and Pb, and somewhat elevated levels of Cu, Zn and TOC, in the downstream station (S-TLP-3) compared to the reference station (R1). There was no major difference with regards to Hg levels between the two stations. The geochemical data have been normalised against TOC-content and grain-size (content of material with grain-size less

than 0.063 and 0.030 mm) in order to compensate for, and evaluate the significance of these parameters. These parameters are generally considered to be important for the contents of trace metals in sediments because of the adsorption of such elements to fine-grained matter and organic matter. Normalisation of Ba against these parameters may have a limited value, but is nonetheless shown in order to supplement the other elements. The geochemical data are listed in Table 1. The analytical method used for dissolution of the geological material (NS4770, 7N HNO₃) has limitations when high concentrations of barium are involved (Hartley 1996). The maximum amount of Ba which can be extracted using the NS4770 method is expected to be 10.000 mg/kg (Ødegård 1996). Many sample types may have S present in the form of sulphates other than barite, or in the form of sulphides or other compounds which can form SO₄²⁻ -ions during the extraction. In such cases the maximum amount of Ba which can be determined will be less than 10.000 mg/kg, since the amount is regulated by a constant ion product (Ba²⁺)(SO₄²⁻) (Ødegård 1996).

Station S-TLP-3

A bivariate plot with element concentrations versus depth in the core (Fig. 7) shows that:

- Ba and Pb has a marked increase from c. 4 cm upward, with a peak in the 0.75-1.25 cm interval, and decrease towards the top.
- Ba contents are low (at background contents) from 15 cm downward. Slightly increased contents occur in the 4-15 cm interval, probably due to bioturbation.
- Cu, Zn, Hg and TOC increase from 4 cm and upwards. The Hg increase is very irregular.
- Cu and Zn have higher contents at 25 and 30 cm levels than in the upper 5 cm.
- TOC contents at the 25 and 30 cm levels are roughly similar to those at the surface.

Normalisation against the TOC content (Fig. 8) showed that:

- Pb is clearly elevated in the upper 4 cm, and exceeds the Pb contents at 25 and 30 cm.
- Cu and Zn show increased contents from 4 cm and upwards, but the contents are lower than at 25 and 30 cm.
- Hg shows an increase in the upper 4 cm, and slightly exceeds the contents at 25 and 30 cm.

Normalisation against the content of material finer than 0.063 mm (Fig. 9A) showed that:

- Pb is clearly elevated in the upper 4 cm, and exceeds the Pb contents at 25 and 30 cm.
- Cu and Zn do show increased contents from 4 cm upward, slightly exceeding the Cu and Zn contents at 25 and 30 cm.
- Hg shows an increase in the upper 4 cm, with contents exceeding the 25 and 30 cm contents.

Normalisation against the content of material finer than 0.030 mm (Fig. 9B) reduced the contents of Cu, Zn and Pb at the 20-30 cm levels to lower values than at 5-10 cm levels.

Station R1-A

A bivariate plot with element concentrations versus the depth in the core (Fig. 10) showed that:

- Ba and Pb has a fairly marked increase from 4 cm upward, but the maximum Pb contents in the uppermost part only equals the Pb contents at 25 and 30 cm.
- Ba contents are low (at background contents) from 3.25 cm downward.
- Cu and Zn increase weakly from 4 cm upward, but the Cu and Zn contents are considerably higher at 25 and 30 cm levels than in the upper 4 cm
- Hg increases in a fairly regular manner from c. 4 cm upward, and the Hg contents in the upper 4 cm are higher than at 25 and 30 cm.
- TOC contents increase from 5 cm upward, but are higher at 25 and 30 cm.

Normalisation against the TOC content (Fig. 11) showed that:

- Pb has an increasing trend in the upper 4 cm, but the maximum Pb contents in the uppermost part only equals the Pb contents at 25 and 30 cm.
- Cu and Zn show a generally decreasing trend.
- Hg shows an increase in the upper 5 cm, exceeding the 25 and 30 cm content.

Normalisation against the content of material finer than 0.063 mm (Fig. 12A) showed that:

- Pb is clearly elevated in the upper 4 cm, and exceeds the Pb contents at 25 and 30 cm.
- Cu contents are rather stable from 15 cm upward, and with higher contents in the 20-30 cm interval.
- Zn increases slightly in the upper 4 cm, but these contents are considerably lower than Zn contents in the 20-30 cm interval.
- Hg shows an increase in the upper 5 cm, clearly exceeding the 25 and 30 cm content.

Normalisation against the content of material finer than 0.030 mm (Fig. 12B) reduced the Cu and Zn contents at the 20-30 cm levels to contents roughly similar to the Cu and Zn contents in the 0-5 cm interval. For Pb and Hg, the normalisation gave rise to a more pronounced upward increasing trend in the 0-10 cm interval.

4. DISCUSSION AND CONCLUSIONS

Clearly elevated levels of Ba and Pb (Fig. 13) are found in the S-TLP-3 station downstream Snorre. The similarity of the temporal trends for these elements suggests that barite from discharges of drilling mud is the main source for the elevated Pb levels. The normalisation of the trace elements against TOC and grain-size demonstrates that the elevated levels of Pb is influenced, but in no way controlled by these factors.

The Ba and Pb contents in the sediments increase from c. 1960, reach peak levels in the 1980-1990 interval, and slightly decrease (c. 5%) towards the surface (Fig. 13). It should be noted that the maximum concentrations of Ba recorded in the top sediments are close to the limit of barite solubility when NS4770 methods are used, and it is questionable if this decrease is really significant (M. Ødegård pers. comm). The elevated Ba and Pb contents prior to 1980, when discharges of drilling muds in the Snorre field started, may be due to bioturbation bringing the contaminants downward in the sediment (c. 1.5 cm). The slightly fluctuating sedimentation rates in the 1960-1990 interval (Fig. 6A) may indicate some disturbance of the sediments in this interval (upper 3.5 cm). The peak levels in the 1980-1990 interval and subsequent slight decrease towards the present would tend to indicate that the largest discharges occurred between 1980 and 1990 overlapping in time with the exploration drilling, and with a subsequent decrease. However, the main discharges are reported to have occurred after 1990, with the maximum discharges in 1993 and 1994. The reason for this discrepancy is not fully understood. Some slight changes in the sedimentary regime is indicated by the somewhat fluctuating median diameter in the 0-4 cm interval (Fig. 2B). This is in contrast to the stable median diameters in the same interval in the R1-B core (Fig. 2B). Resuspension of contaminated material may be considered, but is not clearly indicated by the ^{210}Pb and ^{137}Cs results. Changing oceanographic conditions, influencing the main area of drilling mud deposition over a time scale of years may also be considered. Finally, it should be remembered that the slight changes of Ba concentrations may not be significant, due to the limited barite solubility when NS4770 methods are employed.

Elevated levels of Ba and Pb are also found in the reference station (Fig. 13), but in considerably lower concentrations. The data suggests a background level of c. 50 mg/kg for Ba, while the concentration in the surface sediment is 562 mg/kg. It should be noted that a comparison between the Ba concentrations in fine-grained sediments (clay+silt > 90%, and with a clay:silt ratio >1) from Skagerrak, using partial dissolution according to NS4770 as in this investigation, and total dissolution using hydrofluoric acid, showed significant differences (Longva & Thorsnes, in press). The difference between the concentrations derived from the partial and total dissolution techniques was in the order of 300 mg/kg, for sediments with Ba content less than 1000 mg/kg. This indicates that the factor of 10 between surface (c. 500 mg/kg) and background concentrations (c. 50 mg/kg) indicated by the data above should be treated with caution, even though grain-size differences may certainly influence the difference between the concentrations yielded by these techniques. Still, the surface enrichment of Ba is considerable, and indicates that the discharges from the drilling activity is distributed over a considerable area, and not only downstream. A contribution from other installations than Snorre is also likely. This is in line with Olsgaard & Gray (1995) who suggested that parts of the drilling muds initially deposited close to the platforms may be resuspended and distributed over wide areas. It is also consistent with the modelling of Rye (1996), indicating that substantial parts of the discharged drilling muds contains barite particles with a sufficiently

small grain-size to be transported in suspension, thus allowing a wide distribution. Elevated levels of barium in recently deposited sediments in the Skagerrak also indicate that barite from discharges may be spread over large areas (Longva & Thorsnes, in press).

Elevated levels of Cu and Zn in the S-TLP-3 station sediments, increasing from c. 1970 (Fig. 13) indicate a certain influence from discharges, but even the maximum levels are lower than the levels found in the sediments below c. 20 cm. The reason for the comparatively high levels below 20 cm must be sediment composition; a combination of finer grain-size and higher TOC content than in the 0-20 cm layer. Normalisation against TOC and grain-size demonstrates that the upward increase in the upper 5 cm is a result of increased contaminant input.

Very slightly elevated levels of Cu and Zn in the R1 station sediments (Fig. 13) may indicate some input from the drilling activities, but the TOC-normalisation (Fig. 11) rather indicates that this trend is caused by the increased TOC levels in the uppermost sediments.

Elevated levels of Hg occur in both stations (Fig. 13), and there is no significant difference in the surface sediment concentration of Hg between these stations. This indicates that the distribution of Hg occurs differently from the other trace elements if drilling mud discharges is the main input. Alternatively, the main input of Hg is from other sources, such as suspended material transported from the North Sea or atmospheric inputs, or a combination. The dominant ocean current direction towards the southeast suggests that an origin in the North Sea is less likely. The existing data precludes any firm conclusions to be drawn regarding Hg.

The elevated levels of Cu and Zn, but also to some extent Pb and Hg, in the lower layer (below 20 cm) demonstrates the natural variations of trace metal content in the sediments. Older sediments may locally crop out at the sea-bottom, and be mistaken to represent an area of accumulation, while in fact the location is subject to erosion. Sampling in such sediments may yield a false picture of the present concentration of trace metals, and care should be taken to verify that sediments sampled for environmental analysis represent recently and continuously deposited sediments.

The main conclusions to be drawn from this investigation are:

- Clearly elevated contents of Ba and Pb occur in the downstream station S-TLP-3.
- The peak contents of Ba and Pb coincide with the exploration drilling in the 1980s. A slight decrease in Ba and Pb inputs since the 1980s is indicated from somewhat lower surface contents, compared to the peak contents. These trends do not fit entirely with reported discharges, and indicate that the Ba and Pb contents are influenced by resuspension, changed oceanographic conditions or other factors. Analytical limitations (NS4770 method) may also influence this trend.

- The elevated levels of Ba and Pb likely derived from drilling mud discharges in the reference station, clearly indicates that these contaminants may be spread over considerable areas, and are not only deposited downstream in a limited area.
- The comparatively high levels of trace metals in the lower layer, which may represent a considerably older layer separated from the upper layer by a hiatus, underline the significance of geological control when sampling for environmental purposes, and should have a bearing on the design of future environmental programmes.

5. REFERENCES

- Hartley, J.P. 1996: Environmental monitoring of offshore oil and gas drilling discharges - a caution on the use of barium as a tracer. *Marine Pollution Bulletin* 32, 727-733
- Kunzendorf, H., Longva, O. & Paetzel, M. 1996: Recent sedimentation rates across the Norwegian Trench. *Norges geologiske undersøkelse Bulletin* 430, 67-74.
- Longva, O. & Thorsnes, T. in press: Skagerrak in the past and at the present - an integrated study of geology, chemistry, hydrography and micro fossil ecology. *Norges geologiske undersøkelse Special Publication* 8, xx pp.
- Olsgaard, F. & Gray, J. 1995: A comprehensive analysis of the effects of offshore oil and gas exploration and production on the benthic communities of the Norwegian continental shelf. *Marine Ecology Progress Series* 122, 277-306.
- Rye, H. 1996: Miljøeffekter av utslipp av borekjemikalier. Rapport for OLF. *IKU Petroleumsforskning*. Rapport nr. 42.4053.00/01/96.
- Ødegård, M. 1996: The significance of analytical procedure in geochemical and environmental studies. (Extended abstract). *Norges geologiske undersøkelse Bulletin* 427, 100-103.

Figure captions:

Fig. 1. Location of the S-TLP-3 and R-1 stations.

Fig. 2A. Bivariate plot of dry bulk density versus core depth in cm, both cores.

Fig. 2B. Median diameter in micron versus core depth in cm, both cores

Fig. 3. Grain-size distribution for all samples in the S-TLP-3C and R1-B cores. Please note the consistent two-fold division for core S-TLP-3C, and more fluctuating pattern for core R1-B.

Fig. 4. Estimates of sedimentation rates. A: core S-TLP-3A. B: core R1-A.

Fig. 5. Year AD versus depth in cores.

Fig. 6. ^{137}Cs levels in the S-TLP-3A core. Please note the well-defined peak at 1988 level, likely representing input of radioactive material from the Chernobyl accident in 1986.

Fig. 7. Bivariate plot of Cu, Pb, Zn, Hg, Ba and TOC versus the core depth, core S-TLP-3A.

Fig. 8. Bivariate plot of Cu, Pb, Zn, Hg, Ba and TOC normalised against TOC, versus the core depth, core S-TLP-3A.

Fig. 9. Bivariate plot of Cu, Pb, Zn, Hg, Ba and TOC normalised against grain-size, versus the core depth, core S-TLP-3A. A: normalisation against material finer than 0.063 mm. B: normalisation against material finer than 0.030 mm.

Fig. 10. Bivariate plot of Cu, Pb, Zn, Hg, Ba and TOC versus the core depth, core R1-A.

Fig. 11. Bivariate plot of Cu, Pb, Zn, Hg, Ba and TOC normalised against TOC, versus the core depth, core R1-A.

Fig. 12. Bivariate plot of Cu, Pb, Zn, Hg, Ba and TOC normalised against grain-size, versus the core depth, core R1-A. A: normalisation against material finer than 0.063 mm. B: normalisation against material finer than 0.030 mm.

Fig. 13. Bivariate (stratigraphic) plot of Cu, Pb, Zn, Hg, Ba and TOC versus a time axis in years, based on Pb-dating. Both cores are shown.

Tables

Table 1. Geochemical analyses, grain-size, age and physical properties

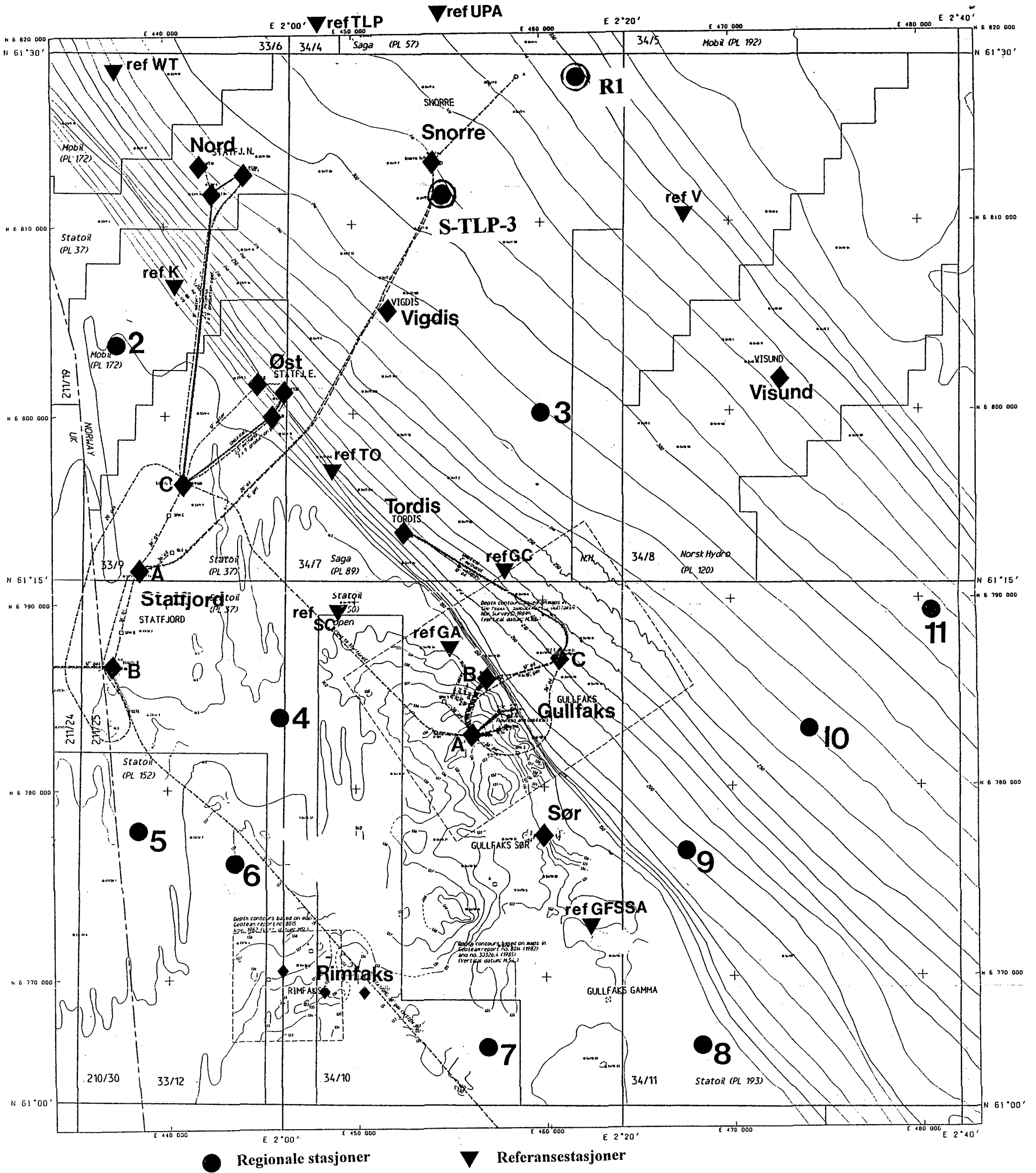


Fig. 1

Dry bulk density versus depth in core

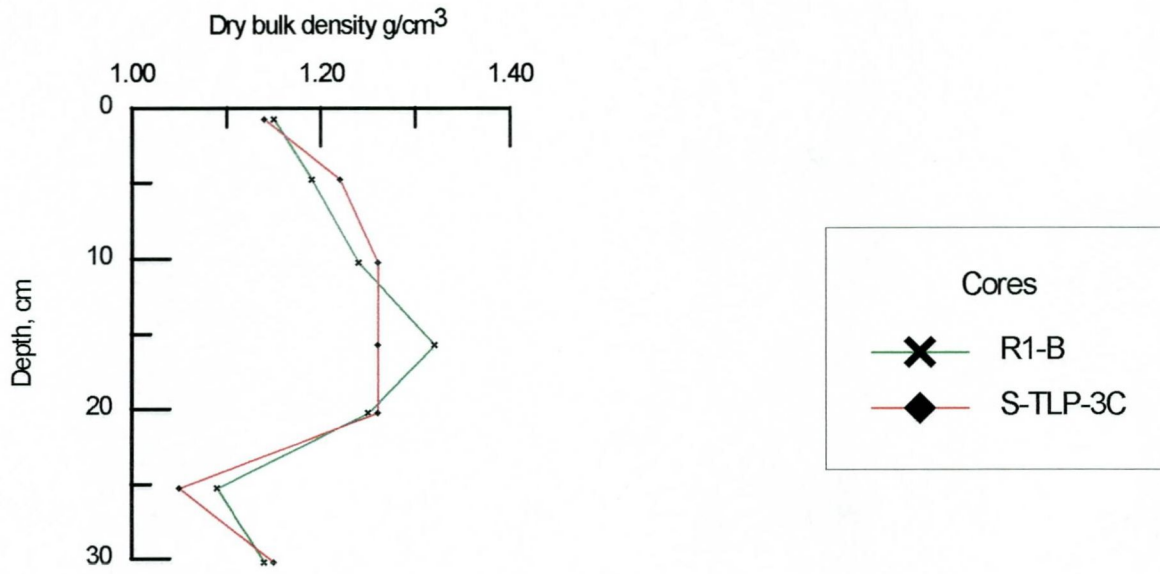


Fig. 2a

Median versus depth in core

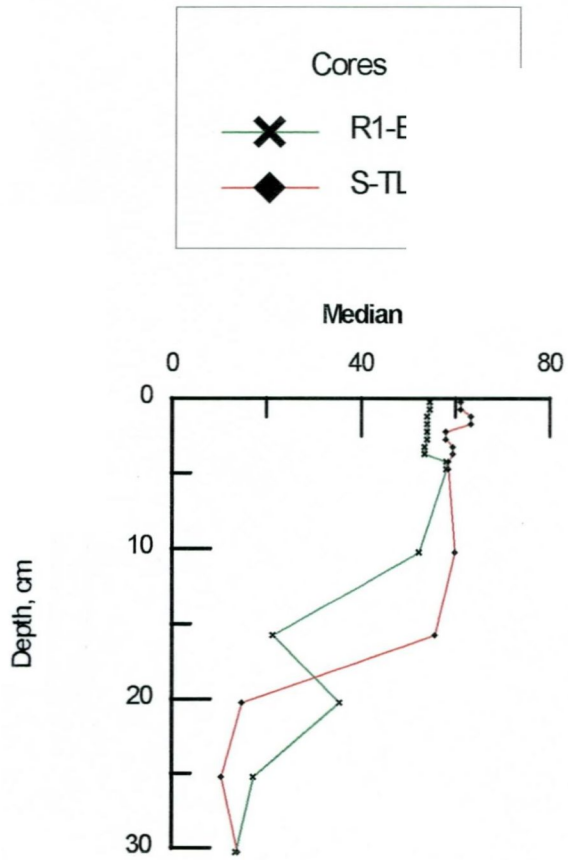


Fig. 2b

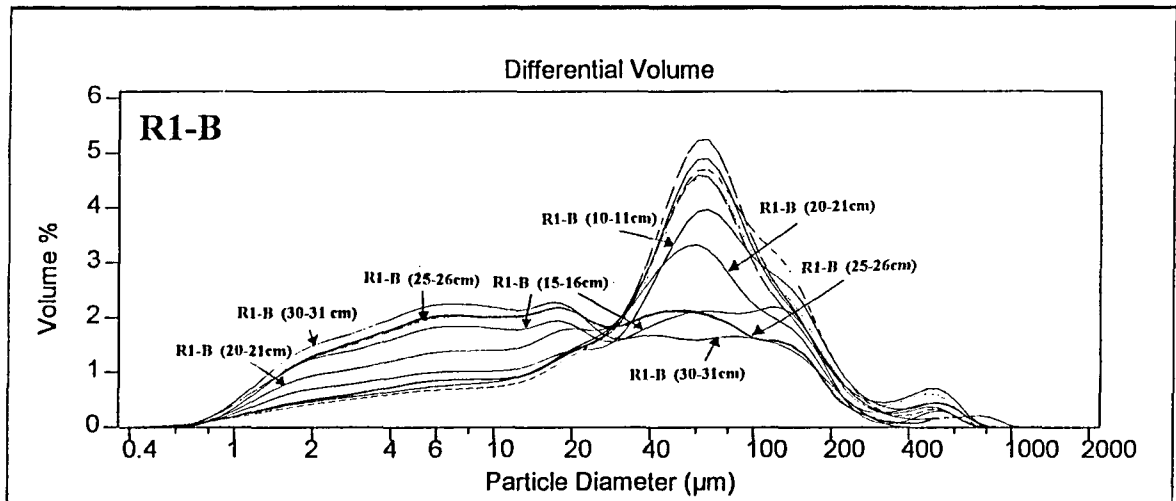
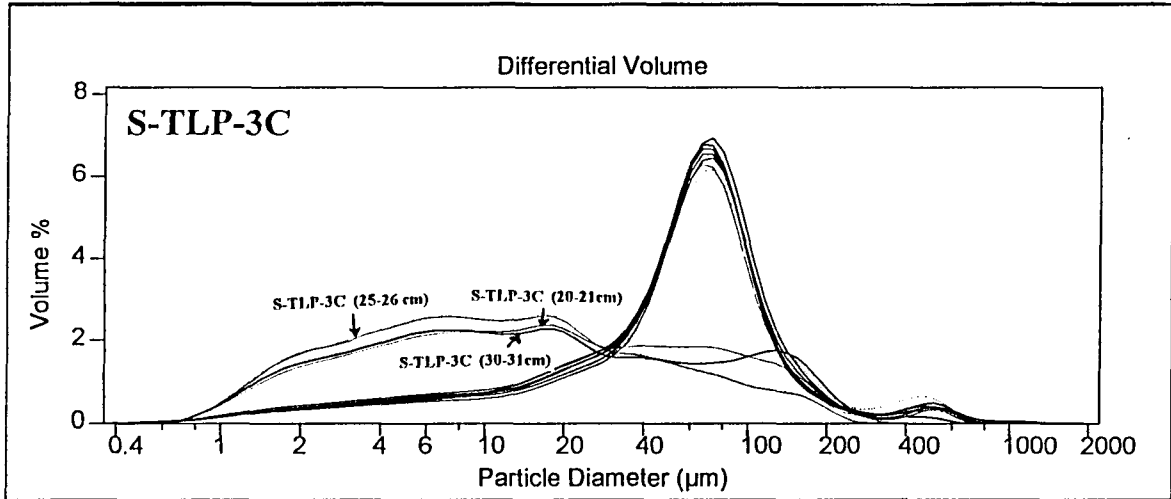


Fig. 3

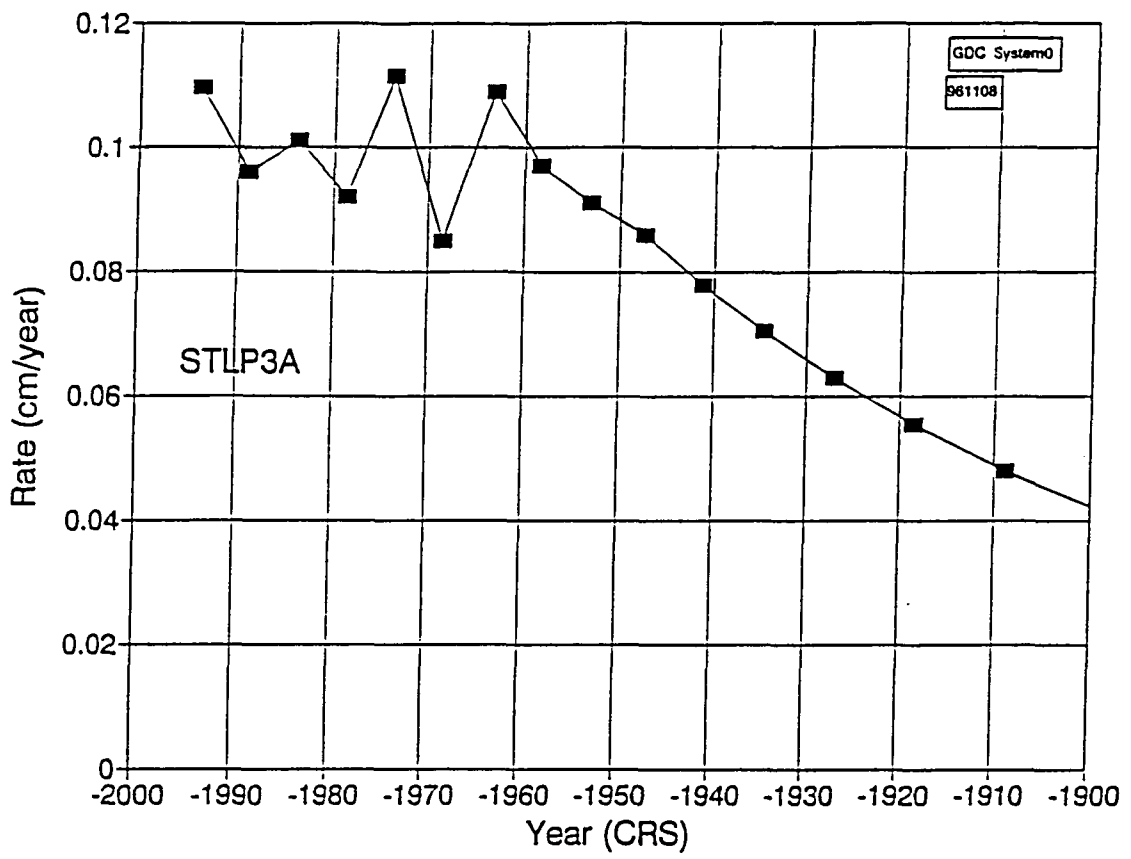


Fig. 4a

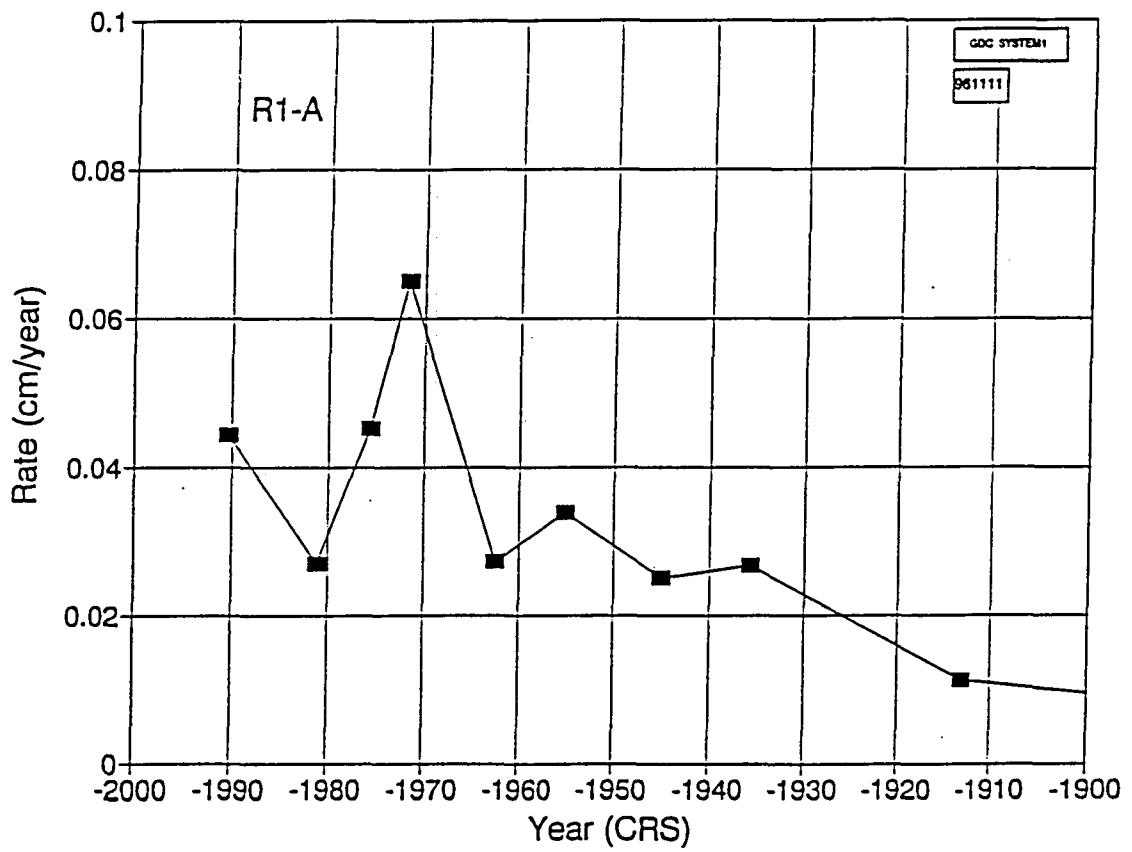


Fig. 4b

R1-A
S-TLP-3A

Year AD versus depth in cores

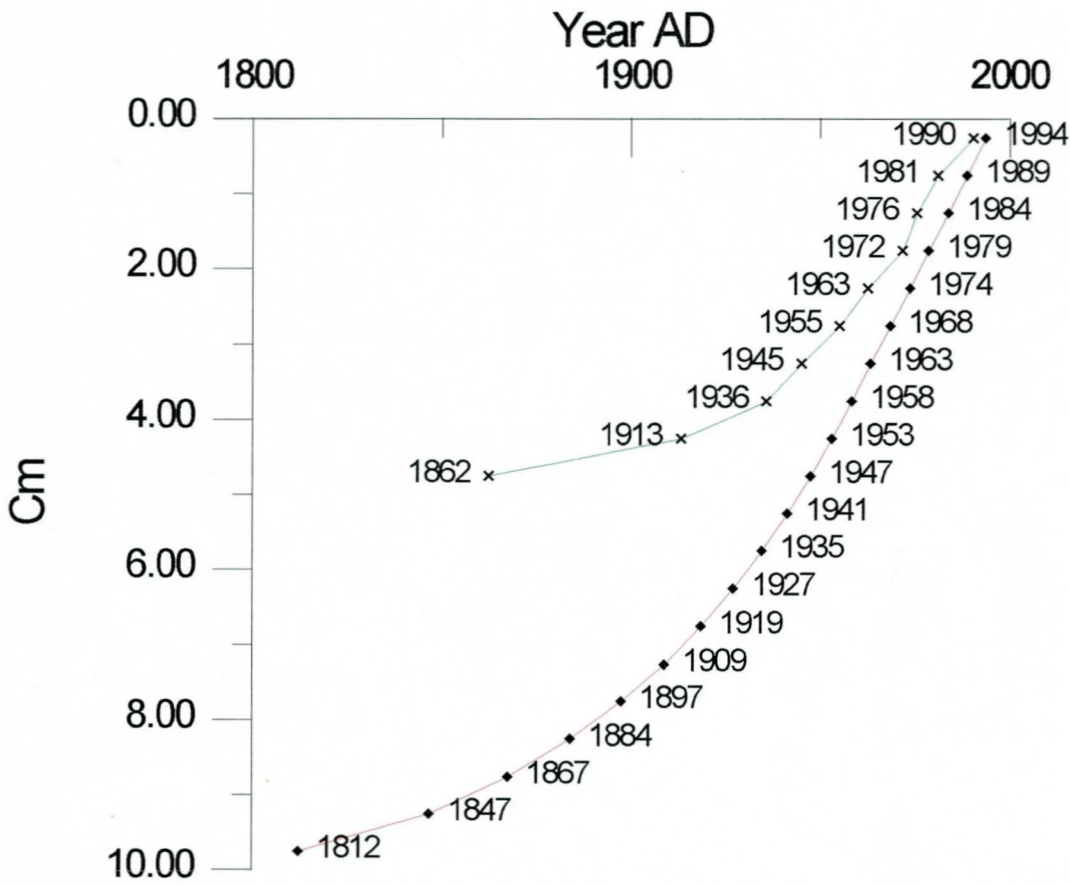
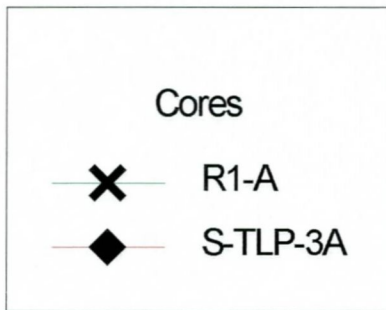


Fig. 5

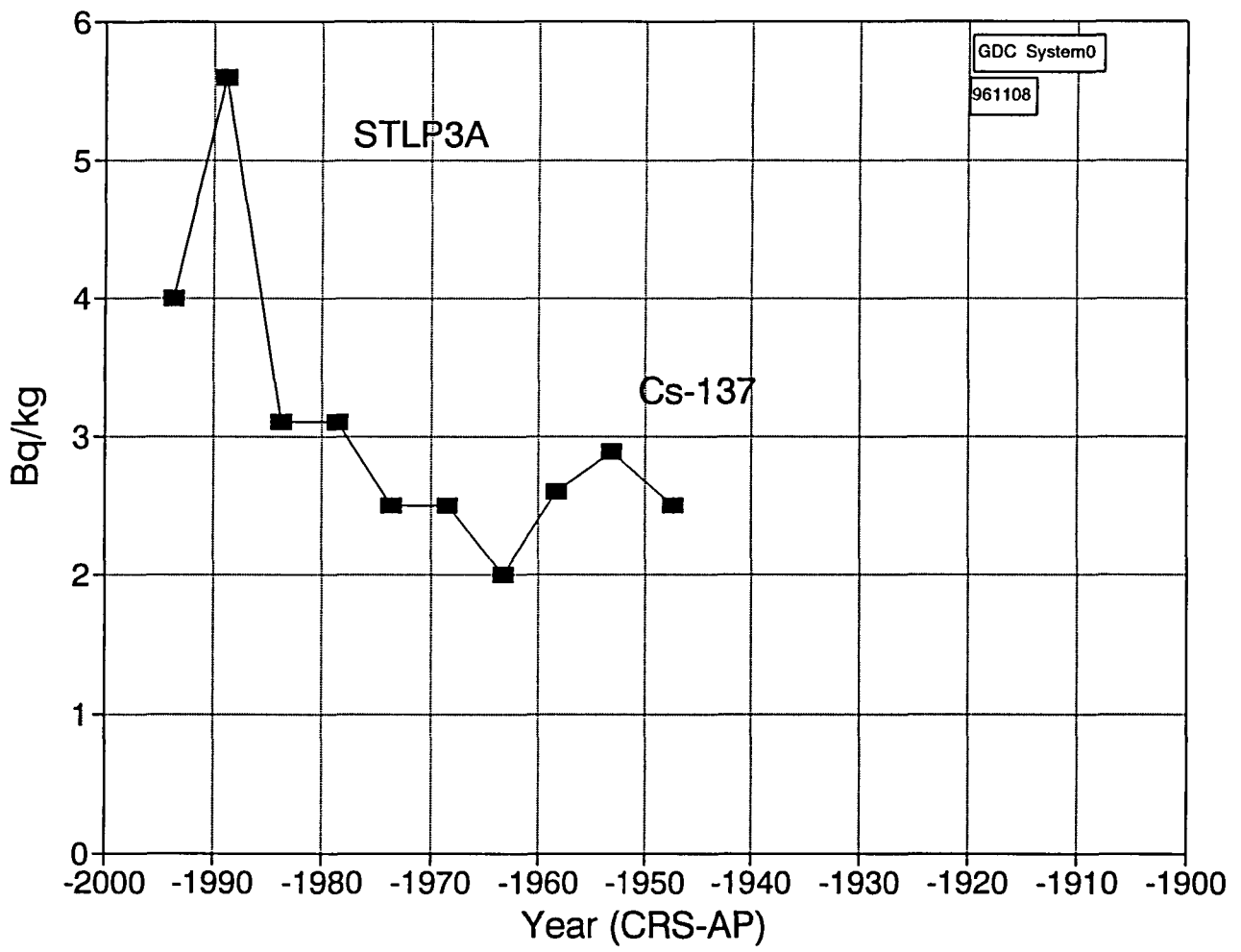


Fig. 6

S-TLP-3A

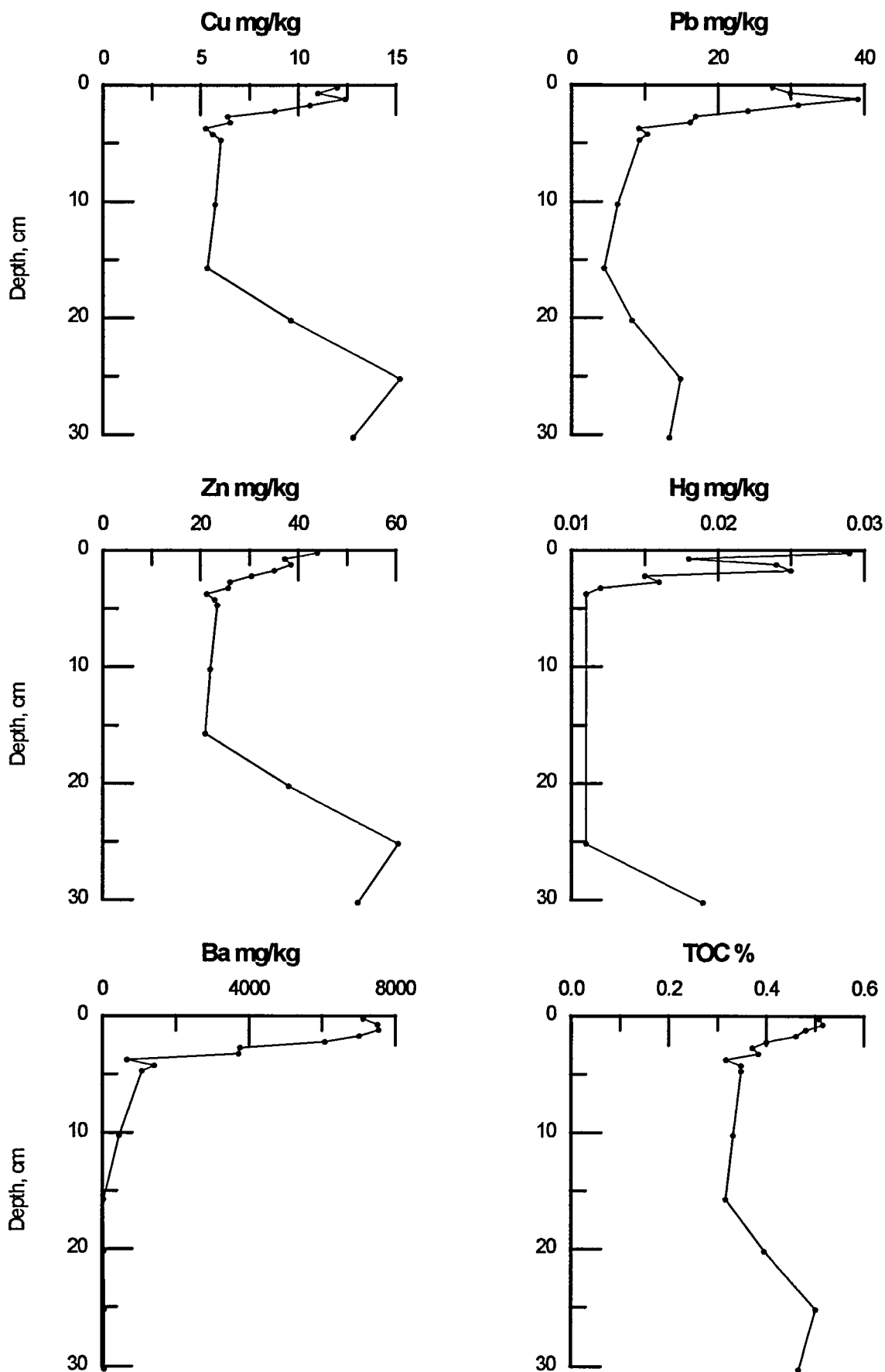


Fig. 7

S-TLP-3A, TOC-normalised

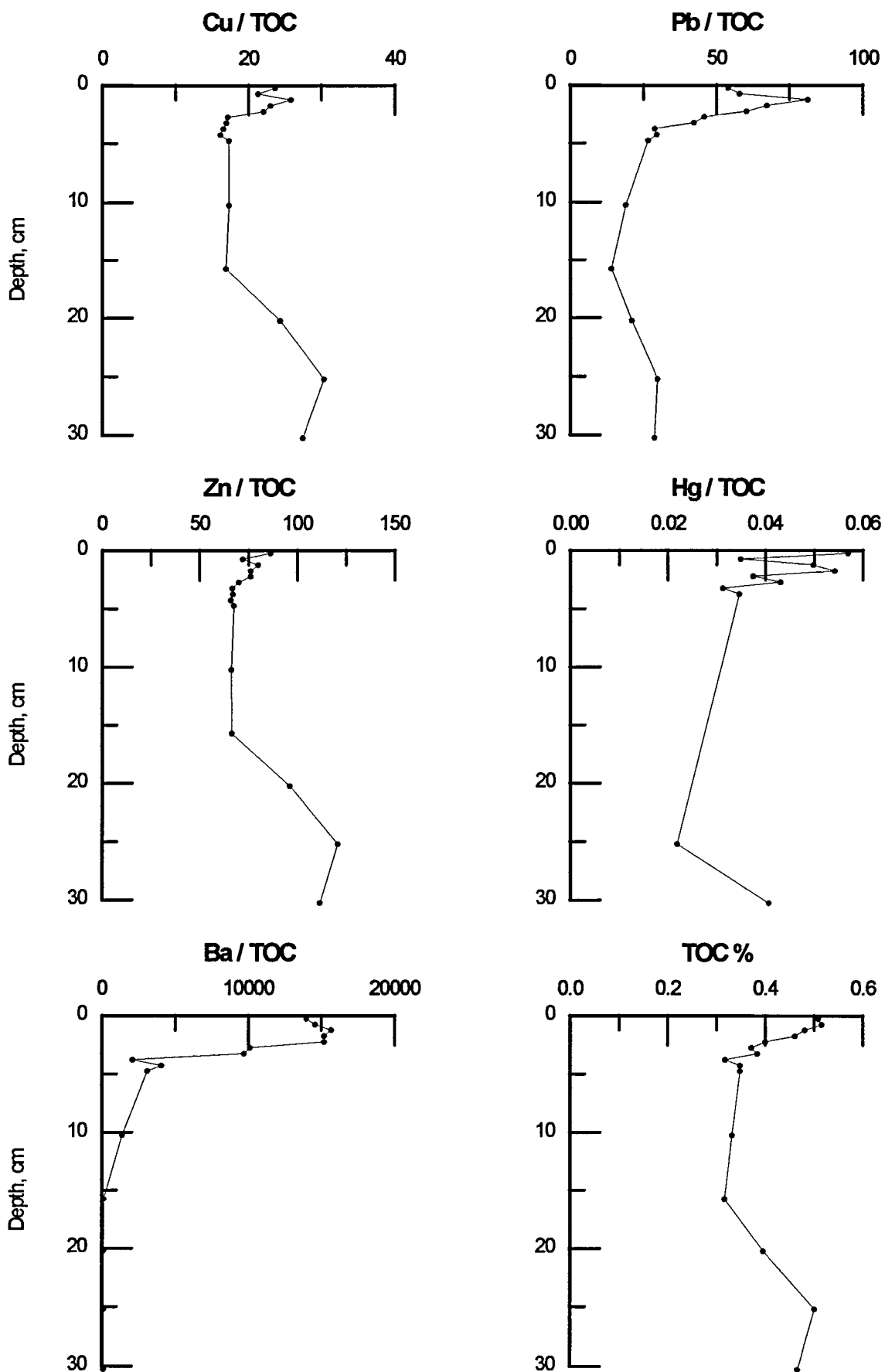


Fig. 8

S-TLP-3A, 0.063 mm normalised

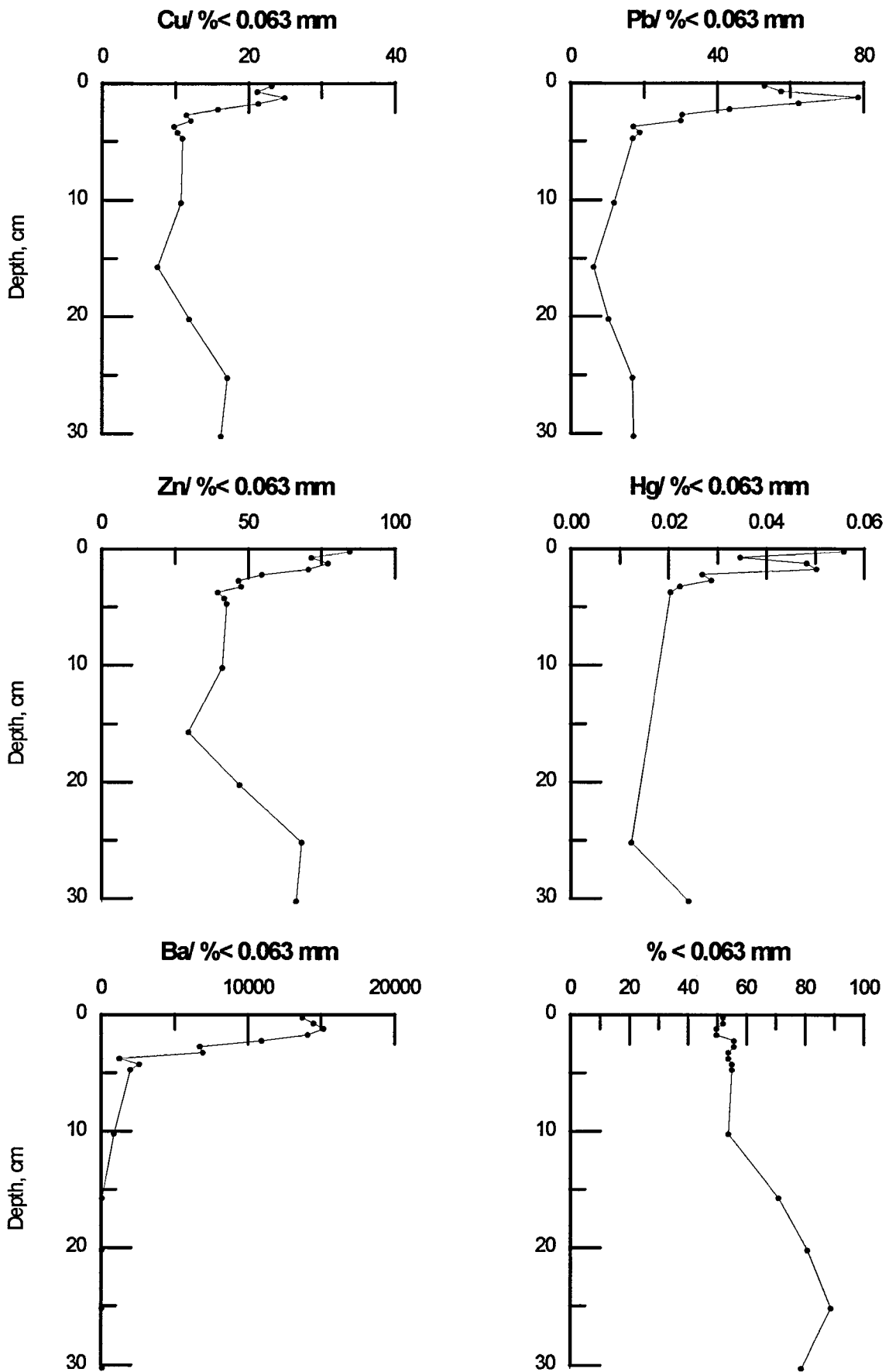


Fig.9a

S-TLP-3A, 0.030 mm normalised

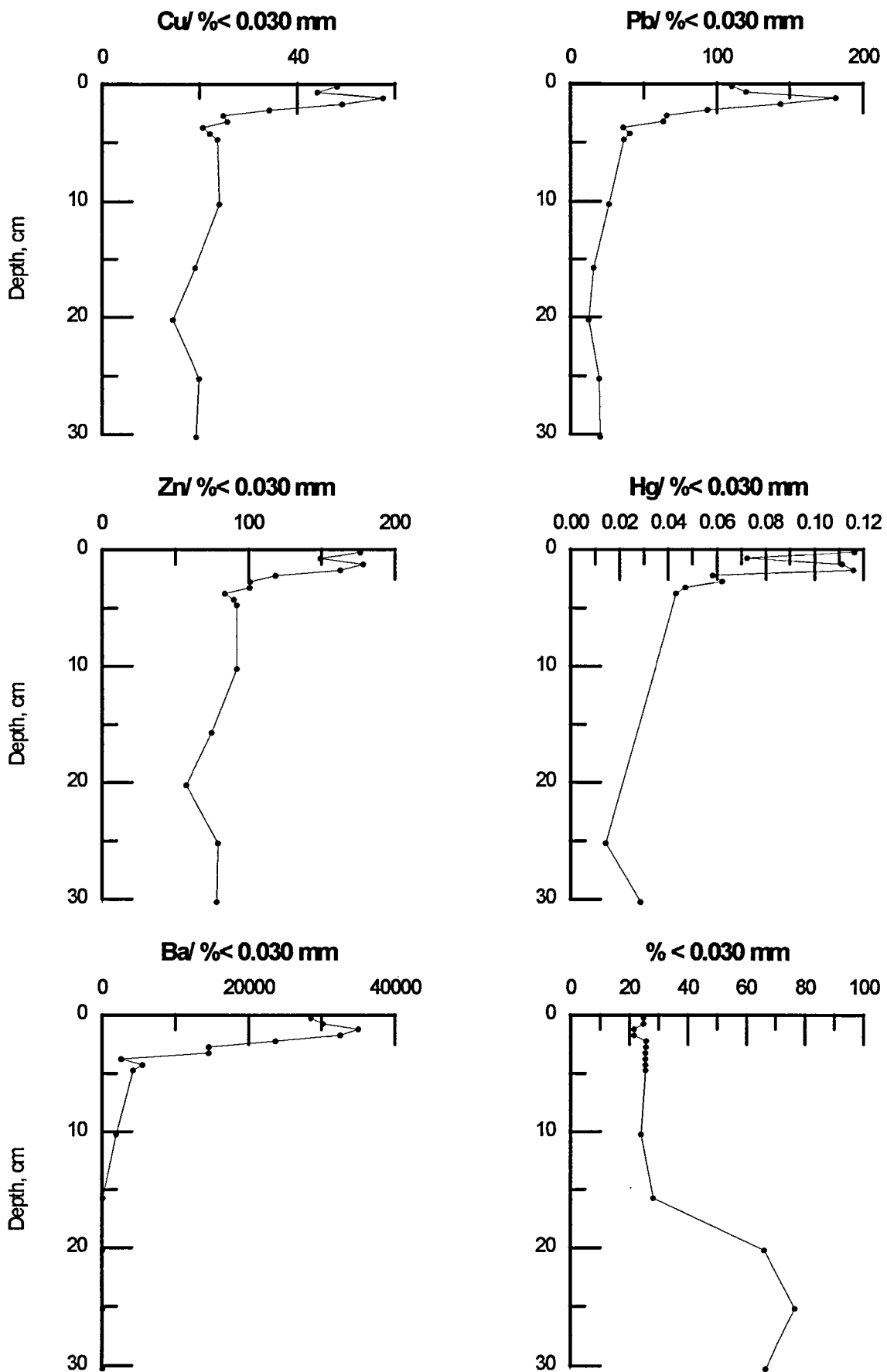


Fig. 9b

R1-A

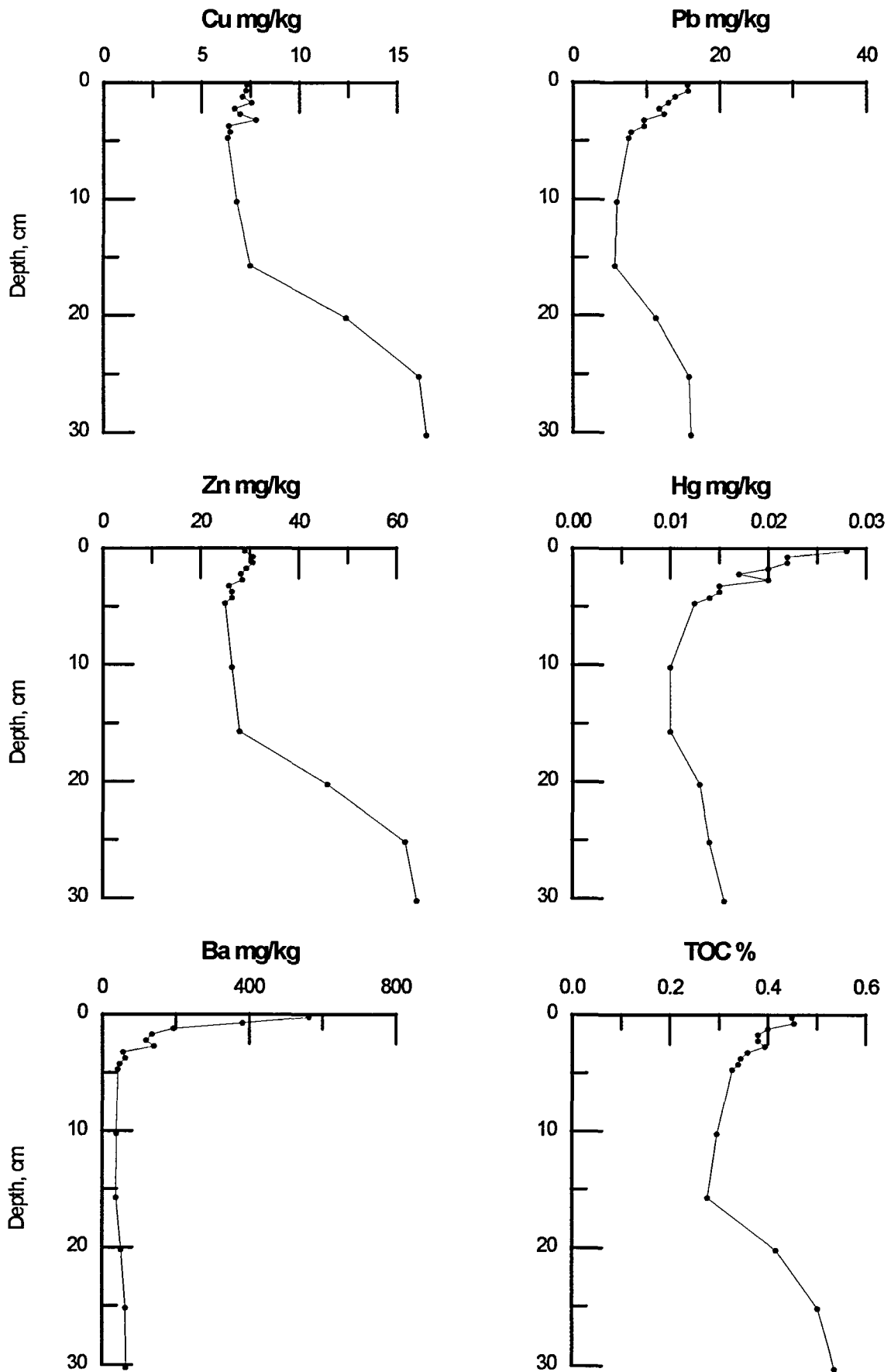


Fig. 10

R1-A, TOC-normalised

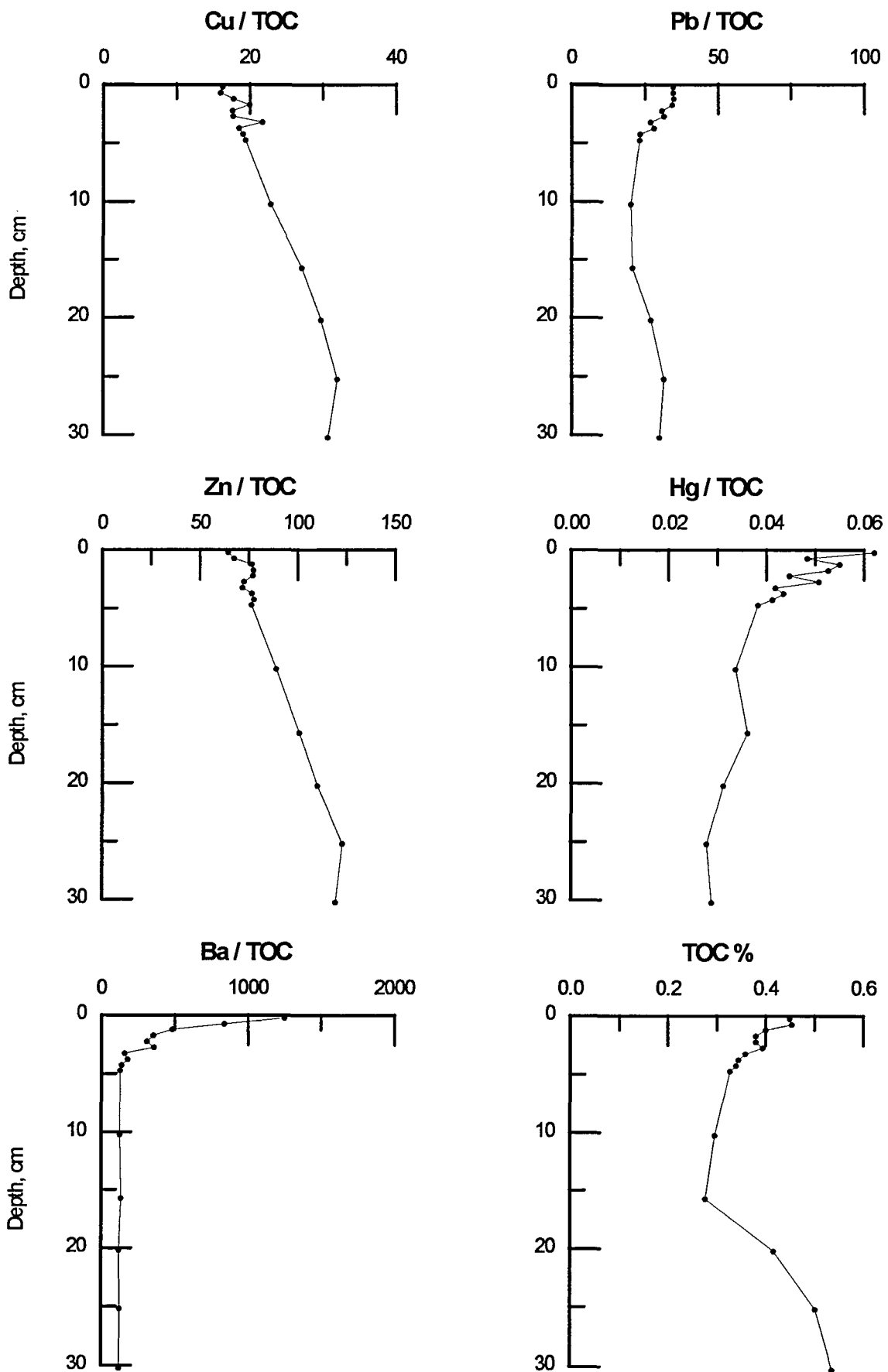


Fig. 11

R1-A, 0.063 mm normalised

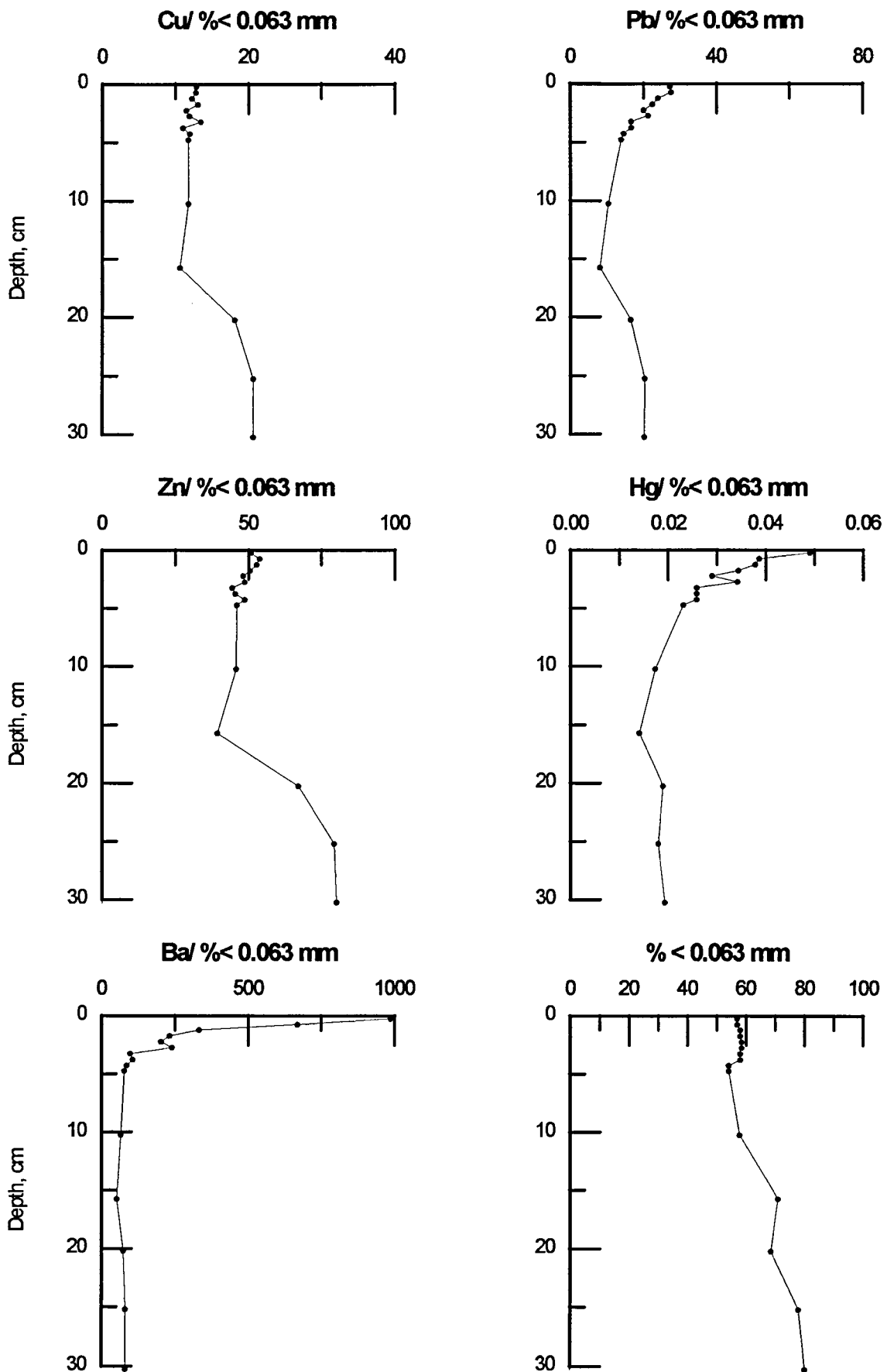


Fig.12a

R1-A, 0.030 mm normalised

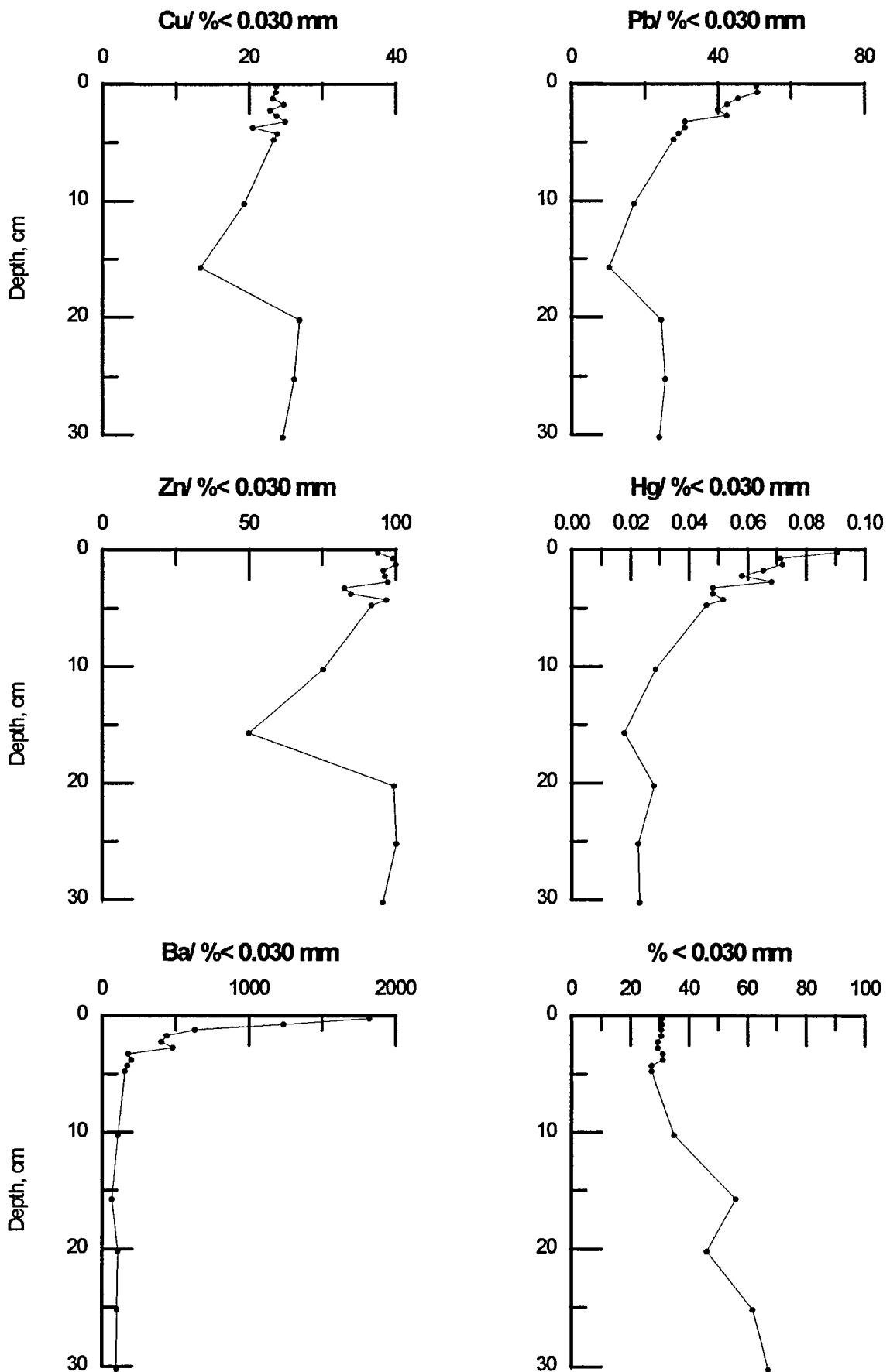


Fig.12b

Stratigraphic plot, cores R1-A and S-TLP-3A

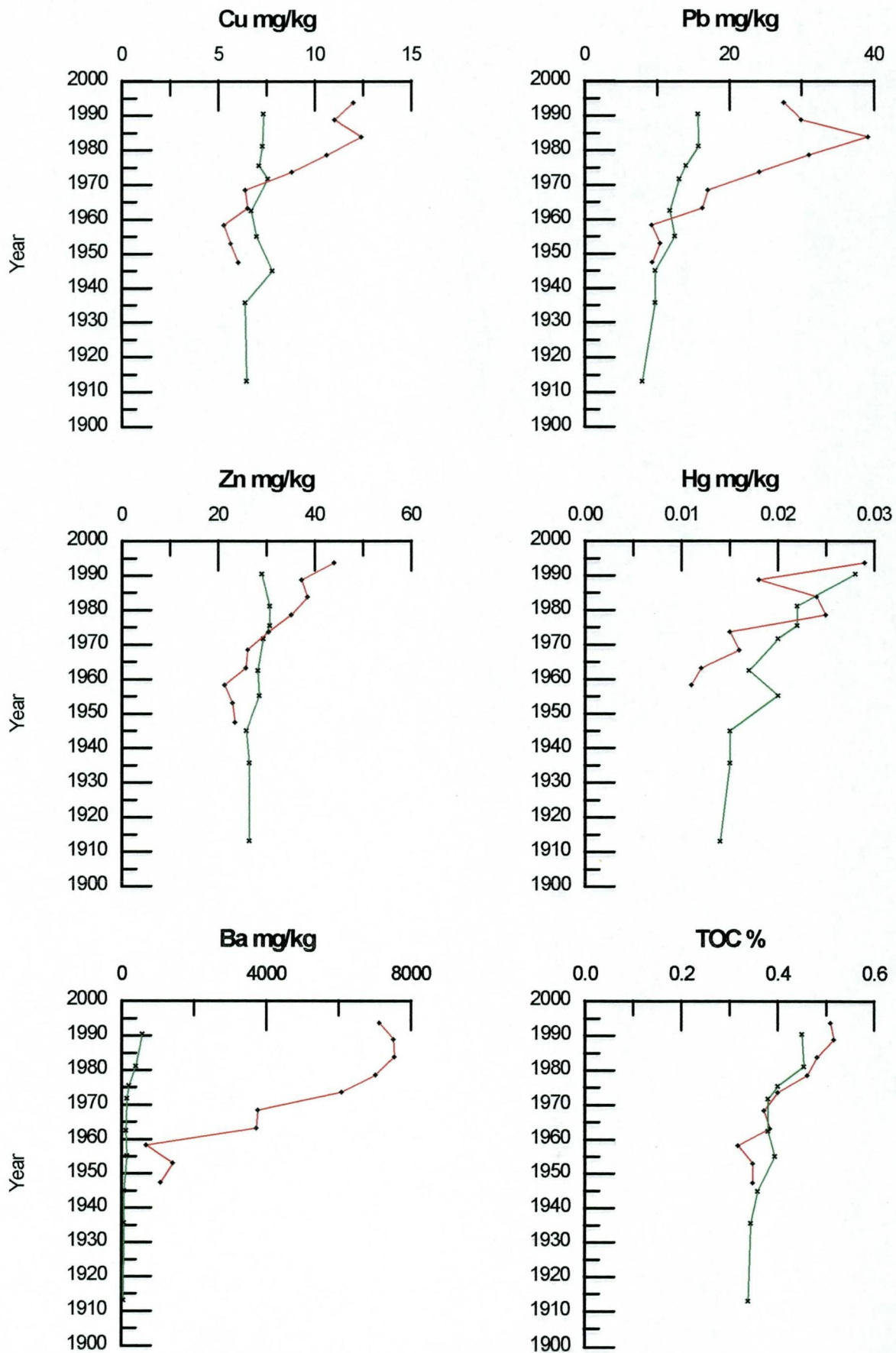
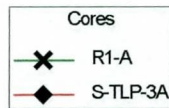


Fig. 13

Lab-id	Core	Interval, cm	Mean, interval, cm	TOC %	Pb mg/kg	Hg mg/kg	Cu mg/kg	Zn mg/kg	Ba mg/kg	Year	0 -2 µm %	0 - 30 µm%	0 - 63 µm %	0 - 125 µm %	Median, µm	Dry bulk density	Wet bulk density
1	R1-A	0-0.5	0,25	0,45	15,6	0,028	7,32	29	562	1990,4	3,29	30,89	56,97	83,51	54,57		
2	R1-A	0.5-1	0,75	0,45	15,7	0,022	7,28	30,6	381	1981,1	3,29	30,89	56,97	83,51	54,57	1,15	1,78
3	R1-A	1.0-1.5	1,25	0,40	13,9	0,022	7,1	30,6	193	1975,5	3,29	30,6	58,05	85,85	53,9		
4	R1-A	1.5-2	1,75	0,38	13	0,02	7,55	29,3	134	1971,7	3,29	30,6	58,05	85,85	53,9		
5	R1-A	2.0-2.5	2,25	0,38	11,7	0,017	6,7	28,2	118	1962,5	3,12	29,31	58,52	87,89	54,01		
6	R1-A	2.5-3	2,75	0,39	12,4	0,02	6,96	28,5	140	1955,1	3,12	29,31	58,52	87,89	54,01		
7	R1-A	3-3.5	3,25	0,36	9,66	0,015	7,77	25,7	55,9	1945	3,31	31,18	57,98	83,74	53,46		
8	R1-A	3.5-4	3,75	0,34	9,65	0,015	6,38	26,4	61	1935,7	3,31	31,18	57,98	83,74	53,46		
9	R1-A	4-4.5	4,25	0,34	7,92	0,014	6,47	26,3	46,3	1913,1	2,83	27,17	54,1	83,1	58,1		
10	R1-A	4.5-5	4,75	0,33	7,56	0,0125	6,34	24,9	41,5	1862,4	2,83	27,17	54,1	83,1	58,1	1,19	1,76
11	R1-A	10-10.5	10,25	0,30	5,97	0,01	6,78	26,4	37,9		4,3	35,07	57,77	82,67	52,15	1,24	1,81
12	R1-A	15-15.5	15,75	0,28	5,74	0,01	7,5	27,9	36,5		6,86	55,99	71,03	86,56	21,31	1,32	1,86
13	R1-A	20-20.5	20,25	0,42	11,3	0,013	12,4	45,9	49,8		5,51	46,24	68,53	87,42	35,43	1,25	1,83
14	R1-A	25-25.5	25,25	0,50	15,8	0,014	16,1	61,8	62,1		7,44	61,71	77,96	91,14	17,31	1,09	1,74
15	R1-A	30-30.5	30,25	0,54	16,1	0,0155	16,5	64,2	64,1		8,53	67,14	80,16	92,04	13,66	1,14	1,73
16	S-TLP-3-A	0-0.5	0,25	0,51	27,5	0,029	12	43,9	7110	1993,7	2,76	24,92	51,96	86,69	61,08		
17	S-TLP-3-A	0.5-1	0,75	0,52	29,9	0,018	11	37,2	7510	1988,8	2,76	24,92	51,96	86,69	61,08	1,14	1,73
18	S-TLP-3-A	1-1.5	1,25	0,48	39,1	0,024	12,4	38,4	7540	1983,8	2,29	21,56	49,8	88,74	63,2		
19	S-TLP-3-A	1.5-2	1,75	0,46	31	0,025	10,6	35,1	7010	1978,6	2,29	21,56	49,8	88,74	63,2		
20	S-TLP-3-A	2-2.5	2,25	0,40	24,1	0,015	8,81	30,4	6080	1973,6	2,52	25,72	55,72	91,86	57,89		
21	S-TLP-3-A	2.5-3	2,75	0,37	17	0,016	6,38	26	3750	1968,4	2,52	25,72	55,72	91,86	57,89		
22	S-TLP-3-A	3-3.5	3,25	0,38	16,2	0,012	6,52	25,6	3720	1963,2	2,56	25,45	53,86	89,85	59,37		
23	S-TLP-3-A	3.5-4	3,75	0,32	9,18	0,011	5,26	21,3	661	1958,3	2,56	25,45	53,86	89,85	59,37		
24	S-TLP-3-A	4-4.5	4,25	0,35	10,3	< 0,01	5,62	22,9	1410	1953	2,33	25,5	54,94	90,92	58,48		
25	S-TLP-3-A	4.5-5	4,75	0,35	9,25	< 0,01	6,02	23,4	1080	1947,4	2,33	25,5	54,94	90,92	58,48	1,22	1,77
26	S-TLP-3-A	10-10.5	10,25	0,33	6,27	< 0,01	5,75	22	455		2,54	23,93	53,69	90,22	59,76	1,26	1,82
27	S-TLP-3-A	15-15.5	15,75	0,32	4,42	< 0,01	5,35	21	30,7		6,86	28,16	71,03	86,56	55,62	1,26	1,83
28	S-TLP-3-A	20-20.5	20,25	0,40	8,26	< 0,01	9,61	38	43,8		7,81	66,23	80,92	93,33	14,87	1,26	1,85
29	S-TLP-3-A	25-25.5	25,25	0,50	14,9	0,011	15,2	60,5	57,5		9,44	76,56	88,83	96,26	10,51	1,05	1,69
30	S-TLP-3-A	30-30.5	30,25	0,47	13,4	0,019	12,8	52,2	52,9		8,35	66,66	78,81	90,16	14,04	1,15	1,83

Table 1. Geochemical analyses, grain -size, age and physical properties.